

The Voltage-Current Characteristic of high T_C DC SQUID: theory, simulation, experiment

Ya. S. Greenberg, I. L. Novikov

Novosibirsk State Technical University, 20 K. Marx Ave., 630092 Novosibirsk, Russia

(Dated: October 15, 2018)

The analytical theory for the voltage-current characteristics of the large inductance ($L > 100\text{pH}$) high- T_C DC SQUIDs that has been developed previously is consistently compared with the computer simulations and the experiment. The theoretical voltage modulation for symmetric junctions is shown to be in a good agreement with the results of known computer simulations. It is shown that the asymmetry of the junctions results in the increase of the voltage modulation if the critical current is in excess of some threshold value (about $8\mu A$). Below this value the asymmetry leads to the reduction of the voltage modulation as compared to the symmetric case. The comparison with the experiment shows that the asymmetry can explain a large portion of experimental values of the voltage modulation which lie above the theoretical curve for symmetric DC SQUID. It also explains experimental points which lie below the curve at small critical currents. However, a significant portion of these values which lie below the curve cannot be explained by the junction asymmetry.

PACS numbers:

I. INTRODUCTION

The new type of superconductors, which has been discovered in the end of the last century by Bednorz and Muller, is widely used in the modern SQUID systems. The majority of high T_C DC SQUIDs are based on the YBCO thin films and have the different types of design^{1,2,3}. However, the adequate theory of the voltage-current characteristic (VCC) of the high- T_C DC SQUID, which would predict its transfer function and energy resolution, still not exists. In recent time intensive computer simulations and theoretical studies have been performed to investigate the dependence of high- T_C DC SQUID behavior on various factors^{4,5,6}, but a marked disagreement of the numerical simulations with experiment is still observed: the experimental transfer functions in many cases are much lower than the values predicted by theory and computer simulations; the white noise is about ten times higher than predicted. This is one of the most important unsolved problems, which seriously hinders the optimization of high T_C DC SQUIDs for applications.

Up to now the high- T_C DC SQUIDs have the significant parameter dispersion, but the reasons of such dispersion are not established. One of the possible reasons for the dispersion could be attributed to the junction asymmetry of SQUID interferometer (unequal critical currents or (and) normal resistances), which for grain boundary junctions is about 20-30 percents due to on chip technological heterogeneity.

Recently, the theory of the voltage-current characteristic of the high T_C DC SQUID, which expands the validity range of the Chesca's analytic theory⁵ on the DC SQUIDs with large inductance $L > 100$ pH and accounts both for the symmetric and asymmetric DC SQUIDs, was developed^{7,8}. The theory is based on the perturbation solution of the two-dimensional Fokker-Planck equation (2D FPE) that describes the stochastic dynamics of DC SQUID in presence of the large thermal fluctuations.

In the paper the results of the analytic theory of VCC of high T_C DC SQUID^{7,8} are compared with the computer simulations and with the experiment. It is shown that the theoretical voltage modulation for symmetric junctions is in a good agreement with the results of known computer simulations. It is also shown that the asymmetry of the junctions results in the increase of the voltage modulation if the critical current is in excess of some threshold value (about $8\mu A$). Below this value the asymmetry leads to the reduction of the voltage modulation as compared to the symmetric case. The comparison with the experiment shows that the asymmetry can explain a large portion of experimental values of the voltage modulation which lie above the theoretical curve for symmetric DC SQUID. It also explains experimental points which lie below the curve at small bias currents (less about than $10\mu A$). However, a significant portion of these values which lie below the curve at larger bias currents cannot be explained by the junction asymmetry.

The paper is organized as follows. In the section II we present in a concise form the main theoretical results for symmetric and asymmetric DC SQUIDs. In Section III we compare theoretical voltage-current characteristics for symmetric DC SQUID with the computer simulations of stochastic dynamical equations of DC SQUIDs which have been made earlier by other authors. In this section we also study in detail the influence of the junction asymmetry on the voltage modulation as compared with symmetric case. In Section IV we compare the theory with experiment and show that the junction asymmetry can explain a large portion of experimental points which lie well above the theoretical voltage modulation curve for symmetric DC SQUID.

II. THE MAIN RESULTS OF THE ANALYTIC THEORY OF VCC OF HIGH T_C DC SQUID

A. Symmetric DC SQUID

We consider a symmetric DC SQUID with equal critical currents of junctions, $I_{C1} = I_{C2} \equiv I_C$, equal normal resistance, $R_1 = R_2 \equiv R$, and loop inductance L . The equations, describing such SQUID, have the following form:

$$\frac{L}{2R} \frac{d\Phi}{dt} = \Phi_X - \Phi - LI_C \cos \delta \sin \varphi + \frac{L}{2} I_{N_-}(t) \quad (1)$$

$$\frac{\Phi_0}{\pi R} \frac{d\delta}{dt} = I - 2I_C \sin \delta \cos \varphi - I_{N_+}(t) \quad (2)$$

where $\Phi_0 = h/2e$ is a quantum of magnetic flux, Φ is a magnetic flux trapped in the interferometer loop, Φ_X is external magnetic flux, I is a bias current, $\varphi = \pi\Phi/\Phi_0$, $\delta = \pi\Delta/\Phi_0$. The quantities $I_{N_{\pm}}(t)$ are independent stochastic variables related to the Nyquist current noise of junctions:

$$\langle I_{N_{\pm}}(t) I_{N_{\pm}}(t') \rangle = \frac{4k_B T}{R} \delta(t - t') \quad (3)$$

where k is the Boltzmann constant, T is the absolute temperature.

The output voltage across SQUID is the low frequency part of the equation (2), which is averaged over the noise:

$$V = \frac{\Phi_0}{2\pi} \left\langle \frac{d\delta}{dt} \right\rangle \quad (4)$$

Thus, the stochastic equations (1), (2) are described DC SQUID behavior in presence of the thermal fluctuations. The solution of these equations depends on the following parameters: screening parameter $\beta = 2LI_C/\Phi_0$, noise parameter $\Gamma = 2\pi k_B T/\Phi_0 I_C$ and dimensionless inductance $\alpha = L/L_F$, where $L_F = (\Phi_0/2\pi)^2/k_B T$ is a fluctuation inductance, equaled 100 pH at = 77 K. But only two of them are independent due to relation $\alpha = \pi\beta\Gamma$.

The known theoretical approaches to the solution of equations (1), (2) are based on the analysis of the equivalent two dimensional Fokker-Planck equation for the distribution function $P(\Phi, \Delta)$:

$$\frac{1}{2R} \frac{\partial P}{\partial t} = \frac{\partial}{\partial \Phi} \left(\frac{\partial W}{\partial \Phi} P \right) + \frac{\partial}{\partial \Delta} \left(\frac{\partial W}{\partial \Delta} P \right) + k_B T \frac{\partial^2 P}{\partial \Phi^2} + k_B T \frac{\partial^2 P}{\partial \Delta^2} \quad (5)$$

where W is a two dimensional potential energy for DC SQUID:

$$W = E_J \left[1 - \cos \varphi \cos \delta - \frac{i}{2} \delta + \frac{(\varphi - \varphi_X)^2}{\pi\beta} \right] \quad (6)$$

$E_J = \Phi_0 I_C / 2\pi$ is a Josephson coupling energy of two junctions in parallel, $i = I/I_C$, $\varphi_X = \pi\Phi_X/\Phi_0$ is a dimensionless external magnetic flux.

At the present time there exist some analytical solutions of equation (5), which are valid at different ranges of β, Γ, α .

1) The exact analytical solution of FPE can be obtained in the small inductance limit ($L \rightarrow 0, \beta \ll 1, \alpha \ll 1$). In this case SQUID is equivalent to a single Josephson junction with normal resistance $R/2$ and critical current $2I_C |\cos \varphi_X|$. The voltage across such single junction is well known and can be obtained from Ambegaokar-Halperin form⁹:

$$\frac{V}{RI_C} = \frac{\pi\Gamma}{p(i, \Gamma, \varphi_X)} \quad (7)$$

where

$$p(i, \Gamma, \varphi_X) = \left[\int_0^{2\pi} e^{-W(y)} dy \int_0^y e^{W(x)} dx - \left(1 - e^{\frac{2\pi i}{\Gamma}} \right)^{-1} \int_0^{2\pi} e^{W(x)} dx \int_0^{2\pi} e^{-W(x)} dx \right] \quad (8)$$

$$W(x) = (i/\Gamma)x + (2/\Gamma)\cos\varphi_X\cos x \quad (9)$$

2) The approximate analytical solution of FPE (5) was obtained in⁵. This solution is valid at $\beta < 0.3$ and relatively high thermal fluctuations level ($\Gamma > 1$).

3) The original method for the solution of equation (5) for SQUID with large inductance ($\alpha \geq 1$) was presented in⁷. The method is based on the perturbation expansion of the solution of 2D FPE (5) over small parameter $\varepsilon = \exp(-\alpha/2)$. The result is the following expressions for voltage V across a SQUID and voltage modulation $\Delta V = V(\phi_X = \pi/2) - V(\phi_X = 0)$:

$$\frac{V}{RI_C} = \frac{2\pi\Gamma}{p(i, 2\Gamma, 0)} - \frac{1}{2}\exp(-\alpha/2)\cos(2\varphi_X)f(i, \Gamma) \quad (10)$$

$$\frac{\Delta V}{RI_C} = \exp(-\alpha/2)f(i, \Gamma) \quad (11)$$

where the value $p(i, 2\Gamma, 0)$ was defined in (8).

According to⁸

$$f(i, \Gamma) = \frac{256\pi^3 i^2 \Gamma^3}{[p(i, 2\Gamma, 0)]^3} B^2 \quad (12)$$

where

$$B = \sum_{n=-\infty}^{n=+\infty} \frac{(-1)^n I_n\left(\frac{1}{\Gamma}\right) I_{n+1}\left(\frac{1}{\Gamma}\right)}{i^2 + 4n^2 \Gamma^2} \quad (13)$$

I_n is a modified Bessel function.

These expressions are valid for $\alpha \geq 1$ and any values of β , and Γ which are consistent with the condition $\alpha = \pi\beta\Gamma$. Therefore, they can be applied for the analysis of a majority of practical high T_C DC SQUIDS with $\Gamma \approx 0.05 - 1$, $\beta \geq 1$, $\alpha \geq 1$. However, it should be remembered that Eqs.(4) and (11) are the approximate expressions which account for the first order term in the perturbation expansion of the voltage over small parameter $\varepsilon = \exp(-\alpha/2)$.

B. Asymmetric DC SQUID

We describe the junction asymmetry in terms of the asymmetry parameters γ and ρ , which are defined according to: $I_{C1} = (1 + \gamma)I_C$, $I_{C2} = (1 - \gamma)I_C$, $R_1 = R/(1 + \rho)$, $R_2 = R/(1 - \rho)$, where

$$I_C = \frac{I_{C1} + I_{C2}}{2}; \quad \gamma = \frac{I_{C1} - I_{C2}}{I_{C1} + I_{C2}} \quad (14)$$

$$R = \frac{2R_1 R_2}{R_1 + R_2}; \quad \rho = \frac{R_2 - R_1}{R_1 + R_2} > 0 \quad (15)$$

The perturbation method, developed in⁷, has been applied to obtain the expressions for the voltage and its modulation across an asymmetric SQUID with large inductance⁸. Corresponding expressions have the following forms:

$$\frac{V}{RI_C} = \frac{V_0}{RI_C} - 8\pi^3 e^{-\alpha/2} \frac{i\Gamma^4}{p_- p_+} \{S \cos(2\varphi_X + t_0) + Q \sin(2\varphi_X + t_0)\} \quad (16)$$

$$\frac{\Delta V}{RI_C} = 16\pi^3 e^{-\alpha/2} \frac{i\Gamma^4}{p_- p_+} \sqrt{S^2 + Q^2} \quad (17)$$

where $t_0 = (i\rho/2\Gamma)\alpha$;

$$V_0 = \pi RI_C \left(\frac{\Gamma}{(1 - \rho)p_-} + \frac{\Gamma}{(1 + \rho)p_+} \right) \quad (18)$$

$$p_{\pm} = \int_0^{2\pi} e^{-W_{\pm}(y)} dy \int_0^y e^{W_{\pm}(x)} dx - \left(1 - e^{\frac{i(1\pm\rho)\pi}{\Gamma}}\right)^{-1} \int_0^{2\pi} e^{W_{\pm}(x)} dx \int_0^{2\pi} e^{-W_{\pm}(x)} dx \quad (19)$$

$$W_{\pm}(x) = \frac{i}{2\Gamma}(1 \pm \rho)x + \frac{1 \pm \gamma}{\Gamma} \cos x \quad (20)$$

The quantities S and Q have the forms:

$$S = \frac{i}{2\Gamma} \left(\frac{1-\rho}{p_+} + \frac{1+\rho}{p_-} \right) B(\rho, \gamma) B(-\rho, -\gamma) \quad (21)$$

$$Q = \frac{B(\rho, \gamma) A(-\rho, -\gamma)}{p_+} - \frac{B(-\rho, -\gamma) A(\rho, \gamma)}{p_-} \quad (22)$$

where

$$A(\rho, \gamma) = \sum_{n=-\infty}^{n=+\infty} \frac{(-1)^n n I_n \left(\frac{1+\gamma}{\Gamma}\right) I_{n+1} \left(\frac{1+\gamma}{\Gamma}\right)}{\left(\frac{i}{2}(1+\rho)\right)^2 + n^2 \Gamma^2} \quad (23)$$

$$B(\rho, \gamma) = \sum_{n=-\infty}^{n=+\infty} \frac{(-1)^n I_n \left(\frac{1+\gamma}{\Gamma}\right) I_{n+1} \left(\frac{1+\gamma}{\Gamma}\right)}{\left(\frac{i}{2}(1+\rho)\right)^2 + n^2 \Gamma^2} \quad (24)$$

For $\alpha \geq 1$ the expressions (16)-(24) are valid at any values of asymmetry parameters ρ and γ and at any values of β and Γ , which are consistent with the condition $\alpha = \pi\beta\Gamma$.

III. VOLTAGE-CURRENT CHARACTERISTICS

A. Symmetric DC SQUID

According to (10), the influence of SQUID inductance on VCC appeared as the reduction of the apparent value of the critical current (Fig. 1). Such behavior is due to the the suppression and masking of the critical current by the significant thermal current fluctuations in the interferometer loop. The more the inductance the more the suppression of the critical current. If $\alpha \gg 1$ the second term on the righthand side of the expression (10) may be neglected and from comparison of (10) with (4) we see that in this limit the DC SQUID is equivalent to a single Josephson junction whose critical current is twice as less as that for the case $L = 0$.

There are two DC SQUID parameters which are easily measured: the bias current, I , and the voltage modulation, ΔV . By the tuning of the bias current the value $I = I_{MAX}$, which corresponds to the maximum of the voltage modulation ΔV_{MAX} , can be found. On the practice this guarantees the maximum of the SQUID transfer function $dV/d\Phi_X$.

As is seen from (11) its righthand side is the product of two terms, one of them $\exp(-\alpha/2)$ depends on the SQUID inductance only, the other one depends on the bias I and critical I_C currents. The first factor describes the suppression of the critical current by the noise current in the interferometer loop. This is similar to the suppression effect in the interferometer loop with a single Josephson junction¹⁵. The second factor describes the critical current suppression by the thermal fluctuations, which is similar to the suppression effect in a single Josephson junction⁹. The factorization allows us to carry the first factor to the left hand side of expression (11), so that we consider below the reduced modulation $\Delta V_R = \exp(\alpha/2)\Delta V/R$, which depends on the critical and bias currents only.

The typical dependence of the reduced voltage modulation on the bias current I at different critical currents is shown in (Fig. 2). The curves, corresponding to the different I_C 's, are shifted along the current axes and for given I_C each dependence $\Delta V_R(I)$ has a well defined maximum $\Delta V_R(I_{MAX}) \equiv \Delta V_{R,MAX}$ at the corresponding value of the bias current.

From the equation (11) for a set of fixed values of I_C we have computed a set of the values of maximum voltage modulation $\Delta V_{R,MAX}$ with the corresponding values of bias current I_{MAX} . In this way we have obtained the table

of values $\Delta V_{R,MAX}(I_C, I_{MAX})$. With the aid of the table we draw the dependence $\Delta V_{R,MAX}(I_C)$, which is shown in Fig. 3. It is obvious, that this curve gives the upper bound of ΔV for any symmetric DC SQUID. The different points on the curve correspond to the different bias currents I_{MAX} , at which ΔV reaches its maximum.

However, as was mentioned above, the critical current of high- T_C interferometer cannot be measured directly with a good accuracy because of large thermal fluctuations. Therefore, it is useful in practice to use the dependence of the maximum modulation signal ΔV_{MAX} on the corresponding value of the bias current I_{MAX} . Such dependence, obtained from the table of values $\Delta V_{R,MAX}(I_C, I_{MAX})$, is shown on Fig. 4. The different points on this curve belong to the different values of I_C . Every point on the curve is the maximum point on the corresponding curve from Fig. 2.

The characteristic feature of these two curves $\Delta V_{R,MAX}(I_C)$ and $\Delta V_{R,MAX}(I_{MAX})$ is the saturation of $\Delta V_{R,MAX}$ at large critical ($I_C > 50\mu A$) and bias currents. From the curve shown on Fig. 3 the critical current can be obtained from the measured value of ΔV_{MAX} . In addition, this dependence allows one to predict the maximum voltage modulation ΔV_{MAX} , if the critical current of a SQUID is known from the direct measurements.

The influence of inductance on ΔV_{MAX} at different values of the noise parameter, Γ is shown on Fig. 5. The curves were calculated from Eq. (11). It can be seen, that the increase of SQUID inductance leads to the reduction of the voltage modulation in accordance with the scaling law $\exp(-L/2L_F)$. In addition, the increase of the noise parameter, Γ also leads to the decrease of the voltage modulation.

B. Critical current

As is known, it is difficult to measure the critical current of high- T_C Josephson junctions with a good accuracy because VCC is washed out by the thermal fluctuations. This problem can be solved, if we relate the critical current with bias current I_{MAX} , which can be measured directly in SQUID scheme. The idea was realized in the paper¹⁴, where, based on the numerical simulations of the paper¹⁶, the following approximate expression for I_{MAX} has been suggested:

$$I_{MAX} = 2I_C \left(1 - \sqrt{\Gamma/\pi}\right) \quad (25)$$

From Eq. (25) the critical current can be expressed in terms of the well measured bias current, I_{MAX} :

$$I_C = \frac{I_{MAX}}{2} + \frac{k_B T}{\Phi_0} \left(1 + \sqrt{1 + \frac{I_{MAX} \Phi_0}{k_B T}}\right) \quad (26)$$

which for $T = 77K$ becomes:

$$I_C = \frac{I_{MAX}}{2} + 0.514 \left(1 + \sqrt{1 + 1.945 I_{MAX}}\right) \quad (27)$$

where I_C, I_{MAX} are in μA .

The Eq. (25) has been obtained for low- T_C junctions¹⁶ and applied to high T_C SQUIDs in¹⁴. Therefore, it is interesting to compare (26) with our theory. As is seen from Fig. 2, the expression (11) establishes a single-valued dependence between the critical current and the bias current. The bias current is the well-measured parameter in SQUID scheme. If I_{MAX} is known from the experiment the expression (11) permits to find the critical current at which the voltage modulation reaches its maximum. From (11) for a set of critical current values, I_C we have found a set of the bias currents I_{MAX} , which give the maximum voltage modulation. The comparison of Drung's expression (27) with our theory is shown on Fig. 6. As is seen from the figure Drung's expression (27) (solid line) and the theory (crosses) give approximately similar results. The deviation between Drung's curve and theoretical points is no more than 10% in the whole range of I_{MAX} 's.

Below we compare the analytical expression (11) with the results of the computer simulations of the stochastic DC SQUID equations (1) and (2), obtained by other authors. The normalized voltage modulation $\Delta V/RI_C$ as a function of the bias current at the different SQUID inductances is shown on Fig. 7. The curves marked by black stars are the theoretical ones, calculated from Eq. (11) (the curves for $L = 94pT$, $L = 157pT$) and from the Ambegaokar-Halperin expressions (7), (8) (the curve for $L = 0$). The curves marked by open circles obtained by computer simulations of exact stochastic equations (1) and (2)¹⁷. All calculations and simulations were made for $T = 77K$ and noise parameter $\Gamma = 1$ ($I_C = 3.23\mu A$). As is seen from Fig. 7, the simulated curves are close to the calculated ones. Therefore, our expression (11) is a good approximation of the exact solution of stochastic equations (1) and (2).

In addition, we compare our theory with the two well known expressions for the maximum transfer function, $V_{\Phi} = dV/d\Phi$ which have been obtained by the empirical fit to the computed values obtained from the simulations of the exact stochastic equations of DC SQUID. The first expression is obtained in⁶ and is valid for $\beta \geq 0.5$, $\Gamma \leq 1$:

$$\frac{\Delta V_{MAX}}{I_C R} = \frac{7.3\beta^{0.15}}{\pi(1+\beta) \left[(80\Gamma\beta)^{0.4} + 0.35(4\Gamma\beta)^{2.5} \right]}. \quad (28)$$

The second one is the widely used expression of Enpuku⁴:

$$\frac{\Delta V_{MAX}}{I_C R} = \frac{4}{\pi(1+\beta)} \exp\left(-3.5\pi^2 \frac{k_B T L}{\Phi_0^2}\right) \quad (29)$$

Here the transfer function was recalculated to ΔV ($\Delta V = V_{\Phi}\Phi_0/\pi$) assuming a sine shape of the voltage-to-flux curve. The comparison of our theory with expressions (28) and (29) for several values of the inductances is shown on Fig.(8).

It is seen, that the theoretical curve (11) and the curve of Enpuku (29) reach the saturation at approximately $I_C > 40\mu A$ while the curve of Kleiner (28) has a constant non vanishing slope. This slope is probably due to the fact that the right hand side of (28) is equal, in fact, to the transfer function V_{Φ} which has actually been calculated in⁶. For relatively high critical currents (small Γ 's) the sine approximation ($\Delta V = V_{\Phi}\Phi_0/\pi$) we made for the shape of the signal is not very good due to the distortion of the signal shape. It is also worth noting that the SQUID inductance affects ΔV_{MAX} in different ways. The Eq. (28) always gives the highest values, except for $\alpha = 2$ for $I_C < 80\mu A$ (Fig. 8d). The Eq. (29) always gives the lowest values, except for $\alpha = 1$ (Fig. 8a). For large inductances $\alpha \geq 2$ the theoretical curve is always higher. The influence of inductance is more pronounced for the voltage modulation given by Eqs. (28) and (29). For example, for $I_C = 100\mu A$ from $\alpha = 1$ to $\alpha = 2.5$ the theoretical voltage modulation is reduced by a factor of two, while the reduction factor for the Kleiner's and Enpuku's expressions is six and nine, respectively.

C. Asymmetric DC SQUID

The numerical simulations of stochastic differential equations, which govern the dynamics of DC SQUID are very time consuming for practical high T_C DC SQUIDS due to the large thermal fluctuations and large loop inductance. This is why in most cases the investigations of asymmetric DC SQUID are restricted to the computer simulations in small inductance limit ($\alpha \ll 1$)^{10,11,12,13,14}. Since our theory is valid for asymmetric SQUIDS with large inductance we cannot compare it with the results of other authors obtained for asymmetric SQUIDS with small inductance.

The practical importance of asymmetric DC SQUIDS is that they have a higher transfer function (the slope of the voltage-to-flux curve) as compared to the symmetric case^{10,11,12,13,14}. This property is generally attributed to the distortion of the voltage-to-flux curve. The shape of this curve significantly differed from the sine shape that results in the high steep of the slope. For large inductance SQUID the voltage-to-flux curve has a sine shape as evident from Eq. (16). Therefore, we carefully studied the influence of the junction asymmetry of large inductance interferometers on the voltage modulation. We have found that in the large range of asymmetry parameters the voltage modulation of asymmetric DC SQUID with large inductance can be significantly higher than that for symmetric SQUIDS.

In principle, the asymmetry parameters γ and ρ are independent of each other and, therefore, they may present in the junctions in any combination. From our calculations we have chosen for presentation here only three types of the junction asymmetry which generally give a correct picture of how the voltage modulation is influenced by any type of asymmetry. Below we present the numerical results for the current asymmetry ($\rho = 0, \gamma \neq 0$), the resistance asymmetry ($\rho \neq 0, \gamma = 0$) and the geometric asymmetry ($\rho = \gamma \neq 0$)¹¹. The effect of different types of the junction asymmetry on the dependence of the voltage modulation on the critical current is shown on Fig. 9 and Fig. 10. As is seen from the figures, the general trends of the asymmetry are the increase of the voltage modulation and non vanishing slope of the curves as compared with the symmetric junctions. The slope being increased with the increase of the asymmetry. For the geometric asymmetry the increase of the voltage modulation is seen in the whole range of the critical currents (Fig. 9), while for the current or resistance asymmetry there exists the range of relatively small critical currents (approximately less than $10\mu A$) where the voltage modulation of asymmetric DC SQUID is lower than that of the symmetric one (Fig. 10). In order to clarify the picture we made a careful study of the dependence of $\Delta V_{R,MAX}$ on the asymmetry parameters at the given values of the critical current. It appears there exists some threshold value of the critical current, approximately in the vicinity of $8\mu A$, which divides the whole range of the critical currents in two parts. Below the threshold the current and resistance asymmetry always leads to the decrease of the voltage modulation as compared to symmetric DC SQUID (Fig. 11a, Fig. 11b). The geometric asymmetry does not change the voltage modulation up till approximately $\rho = \gamma = 0.5$ with the subsequent decrease of the voltage modulation

(Fig. 11c). Above the threshold the curves $\Delta V_{R,MAX}(\gamma, \rho = 0, I_C = const)$ and $\Delta V_{R,MAX}(\gamma = 0, \rho, I_C = const)$ have a clear maximum approximately at the vicinity $\gamma = 0.25$ and $\rho = 0.25$, respectively (Fig. 12a, Fig. 12b). This maximum lies approximately 1.5 times higher a symmetric value for the voltage modulation for current asymmetry and 1.3 times higher a symmetric value for the voltage modulation for resistance asymmetry. It is worth noting that in the wide range of the current asymmetry ($0 < \gamma < 0.7$) or of the resistance asymmetry ($0 < \rho < 0.7$) the voltage modulation is higher than its symmetric value. However, the geometric asymmetry leads to the significant increase of the voltage modulation in the whole range of the critical currents (Fig. 12c).

IV. COMPARISON WITH EXPERIMENT

In order to compare our theory with experiment we took two groups of DC SQUIDS. The first group comprised about 50 SQUIDS which have been chosen before for the same purpose^{18,19}. All of these SQUIDS are single layer ones, using 100 or 200 nm thick $YBa_2Cu_3O_{7-x}$ films deposited by laser ablation onto $SrTiO_3$ bicrystal substrates with 24° or 30° misorientation angles, both having symmetrical configuration. The technology is described in detail in²⁰. The second group comprised 10 bicrystal SQUIDS, which were also single layer ones, using 150 - 200 nm thick $YBa_2Cu_3O_{7-x}$ films deposited by linear hollow cathode sputtering onto $SrTiO_3$ bicrystal symmetrical substrates with 24° misorientation angle²¹. All SQUIDS have $\alpha \geq 1$ and $\Gamma \geq 0.05$ and all measurements were performed in liquid nitrogen at 77 K.

Since the critical current, I_C of a high T_C DC SQUID cannot be measured with a good accuracy due to high level of thermal fluctuations, we here, for the comparison with experiment, use only the quantities, which are measured directly, ΔV_{MAX} and I_{MAX} . The dependence $\Delta V_{R,MAX}(I_{MAX})$ for symmetric SQUID together with experimental points is shown on Fig. 13. It can be seen, that there is a significant deviation of experimental points from theoretical line of symmetric DC SQUIDS. Part of the experimental points which lie above theoretical line can be explained by the junction asymmetry. In order to show this we add to the plot of Fig. 13 the theoretical curves for asymmetric DC SQUID (Fig. 14a and Fig. 14b). We choose a significant asymmetry on these graphs ($\gamma = 0.9; \rho = 0.9$) in order to mark the borders of the possible scattering of the voltage modulation values. In addition, the asymmetry allows one to explain the experimental points which lie below the symmetric line at small bias currents $I_{MAX} < 10\mu A$. Since at small bias currents I_{MAX} is close to I_C (see Eq. (27)) this reduction of the voltage modulation is consistent with the result of section III C where we showed that at relatively small critical currents a junction asymmetry reduced the voltage modulation. Therefore, the junction asymmetry can explain the experimental values of the voltage modulation which lie above the line for symmetric DC SQUID and the points which lie below symmetric line at small bias currents. However, a significant reduction of the voltage modulation, which lies well below a symmetric line in Figs. 13 and 14 cannot be explained by the junction asymmetry. A possible explanation of these points is the presence of relatively large amplitude of a second harmonic in the junction current phase relation¹⁹.

V. CONCLUSION

In the paper we consistently compared the analytical theory for the voltage-current characteristics of the large inductance ($L > 100\text{pH}$) high- T_C DC SQUIDS that has been developed previously^{7,8} with the computer simulations and the experiment. It is shown that the theoretical voltage modulation for symmetric junctions is in a good agreement with the results of known computer simulations. It is also shown that the asymmetry of the junctions results in the increase of the voltage modulation in the large range of critical currents and asymmetry parameters. We compared our theory with the experimental values of the voltage modulation. It appeared that the asymmetry can explain a large portion of experimental values of the voltage modulation which lie above the theoretical curve for symmetric DC SQUID. It also explains experimental points which lie below the curve at small critical currents. However, a significant portion of these values which lie below the curve cannot be explained by the junction asymmetry. From our opinion a possible explanation of these low lying points is the presence of relatively large amplitude of a second harmonic in the junction current phase relation¹⁹.

Acknowledgments

We thank R. Kleiner for providing us with the unpublished results of the numerical simulations shown in Fig. 7 of the paper. We are also grateful to V. Schultze and R. Kleiner for fruitful discussion.

The authors acknowledge the support by the INTAS grant 2001-0809.

- ¹ J. Beyer, D. Drung, F. Ludwig, T. Minotani, K. Enpuku, Appl. Phys. Lett. **72**, 203 (1998) .
- ² K. Park, S.-G. Lee, H.C. Kwon, Y.K. Park, J.-C. Park, IEEE Trans. Appl. Supercond. **5**, 3119 (1995) .
- ³ Q. Jia, F. Yan, C. Mombourquette, D. Reagor, Appl. Phys. Lett. **72**, 3068 (1998).
- ⁴ K.Enpuku, G. Tokita, T. Maruo, and T. Minotani, J. Appl. Phys. **78**, 3498 (1995) .
- ⁵ B. Chesca, J. Low Temp. Phys. **112**, 165 (1998).
- ⁶ D. Koelle, R. Kleiner, F. Ludwig, E. Dankster, John Clarke, Rev. Mod. Phys. **71**, 631 (1999).
- ⁷ Ya. S. Greenberg, Physica **C 371**, 156 (2002).
- ⁸ Ya. S. Greenberg, Physica **C 383**, 354 (2003).
- ⁹ V. Ambegaokar and B. I. Halperin, Phys. Rev. Lett. **22**, 1364 (1969).
- ¹⁰ G. Testa, S. Pagano, M. Russo, E. Sarnelli, EUCAS'99, Inst. Phys. Conf. Ser. **167**, 529 (1999).
- ¹¹ Muller J., S. Weiss, R. Gross, R. Kleiner, D. Koelle, IEEE Trans. Appl. Supercond. **11**, 912 (2001).
- ¹² K. Enpuku, T. Mitonani, A. Kandori, F. Shiraiishi, J. Beyer, D. Drung, F. Ludwig, Jpn. J. Appl. Phys. Pt. 1, **37**, 4769 (1998).
- ¹³ G. Testa, C. Granata, C. Calidonna, C. Di Russo, M. Mango Furnari, S. Pagano, M. Russo, E. Sarnelli, Physica C **368**, 232 (2002).
- ¹⁴ D. Drung, F. Ludwig, W. Muller, U. Steinhoff, L. Trahms, Y.Q. Shen, M.B. Jensen, P. Vase, T. Holst, T. Freltoft, Appl.Phys.Lett. **68**, 1421 (1996).
- ¹⁵ V. A. Khlus, I. O. Kulik, Zhurnal Techn. Fiziki **45**, 449 (1975) (in Russian).
- ¹⁶ R. F. Voss J. Low Temp. Phys. **42**, 151 (1981).
- ¹⁷ R. Kleiner, private communication.
- ¹⁸ Ya. S. Greenberg, V. Schultze, H.-G. Meyer, Physica **C 368**, 236 (2002).
- ¹⁹ I. Ya. S. Greenberg, I. L. Novikov, V. Schultze, H.-G. Meyer, Eur. J. Phys. **B 44**, 57 (2005).
- ²⁰ R. IJsselsteijn, H. Elsner, W. Morgenroth, V. Schultze, and H. G. Meyer, IEEE Trans. on Appl. Supercond. **9**, 3933 (1999).
- ²¹ M. Lindstroem, A Thesis of Master degree, Espoo March 9 (1999).

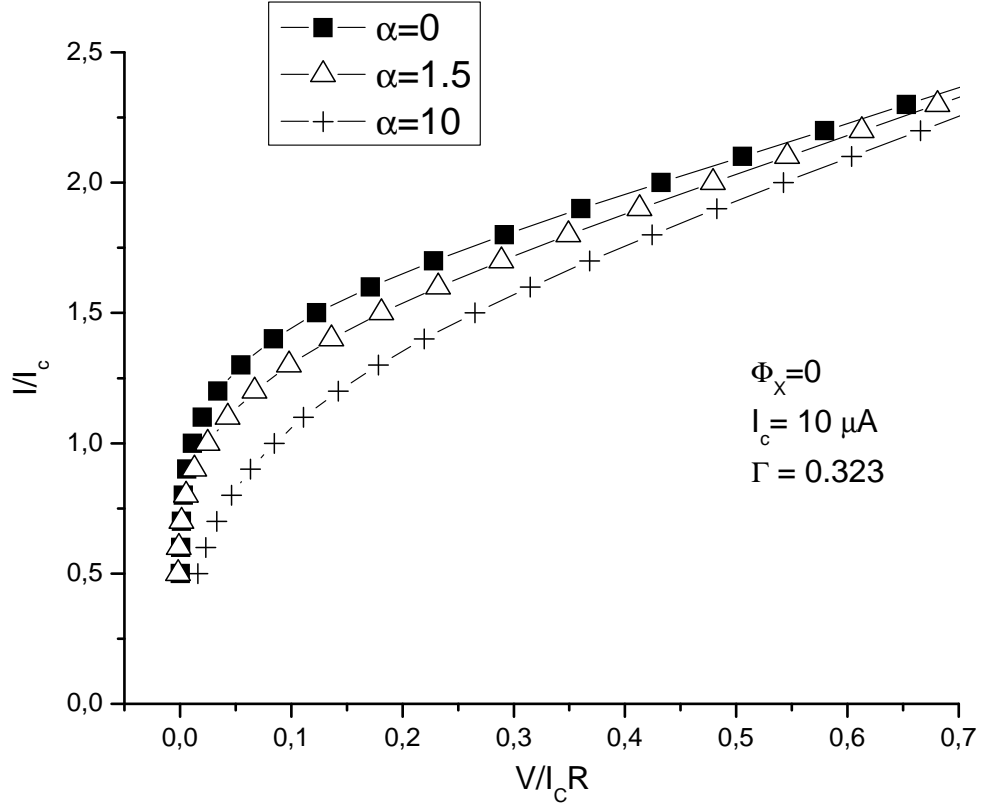


FIG. 1: VCC of symmetric DC SQUID at zero magnetic field and different inductances. $I_C = 10\mu\text{A}$, $T = 77\text{K}$, the curve with $\alpha = 0$ (black box) was calculated from expression (7), the curves with $\alpha = 1.5$ (triangle) and $\alpha = 10$ (cross) were calculated from the expression (10).

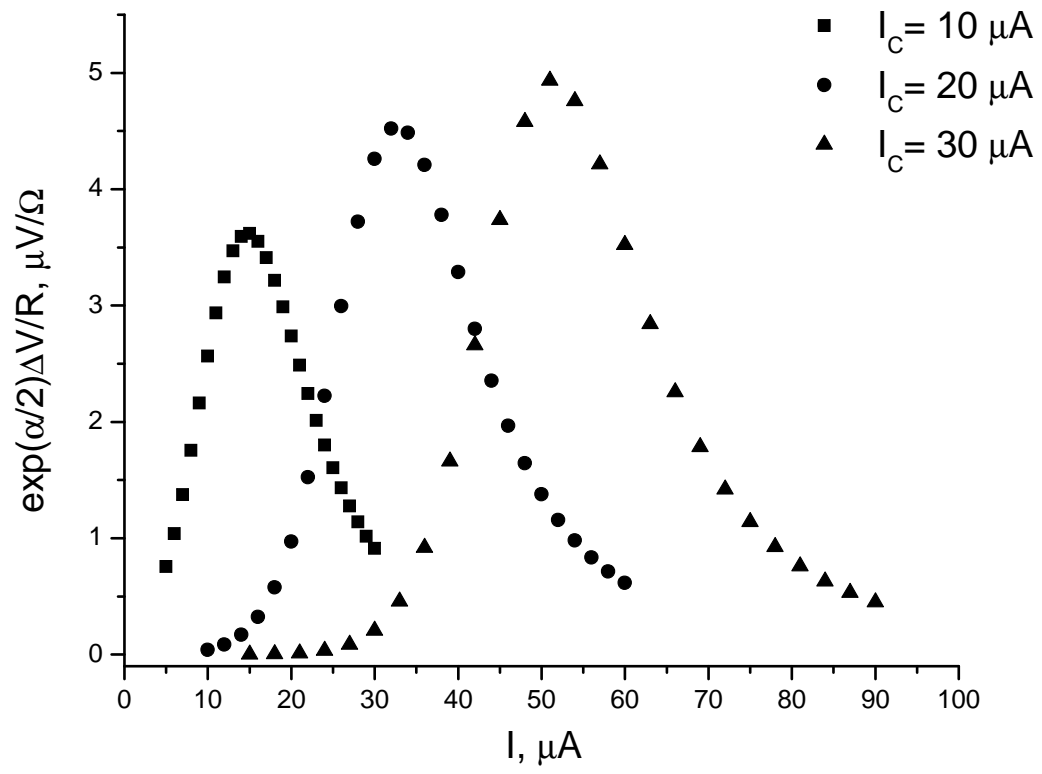


FIG. 2: The reduced voltage modulation vs bias current curves at different values of the critical current for symmetric DC SQUID.

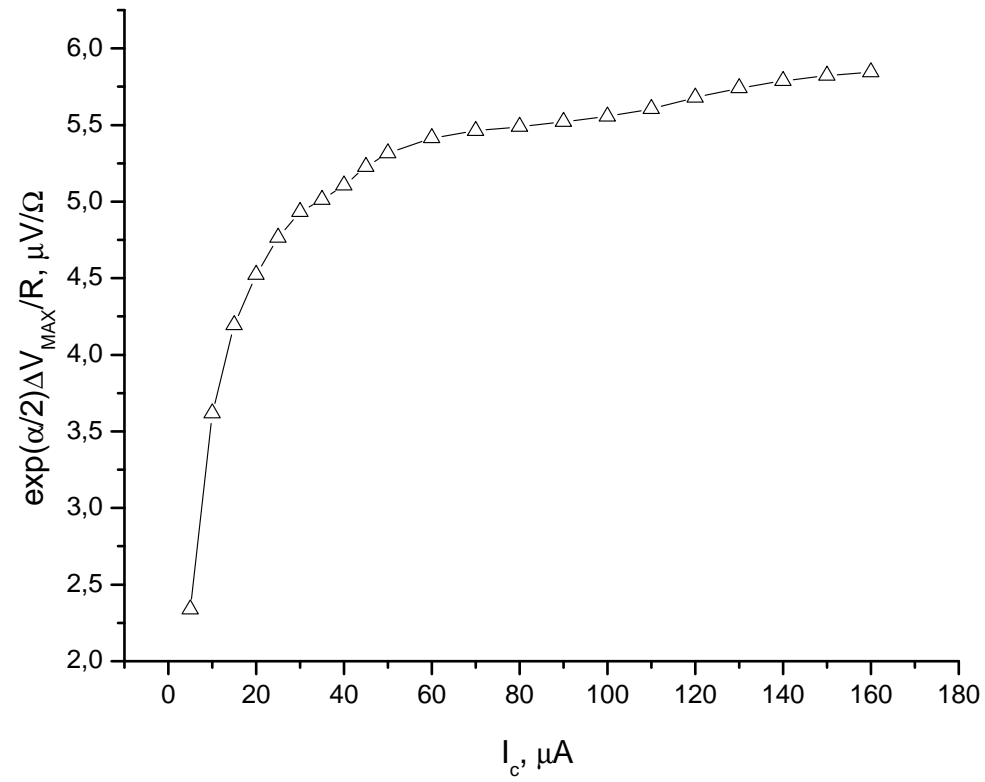


FIG. 3: The maximum value of the reduced voltage modulation, $\Delta V_{R,MAX}$ vs critical current. The different points on the curve correspond to the different bias currents I_{MAX} , at which ΔV reaches its maximum.

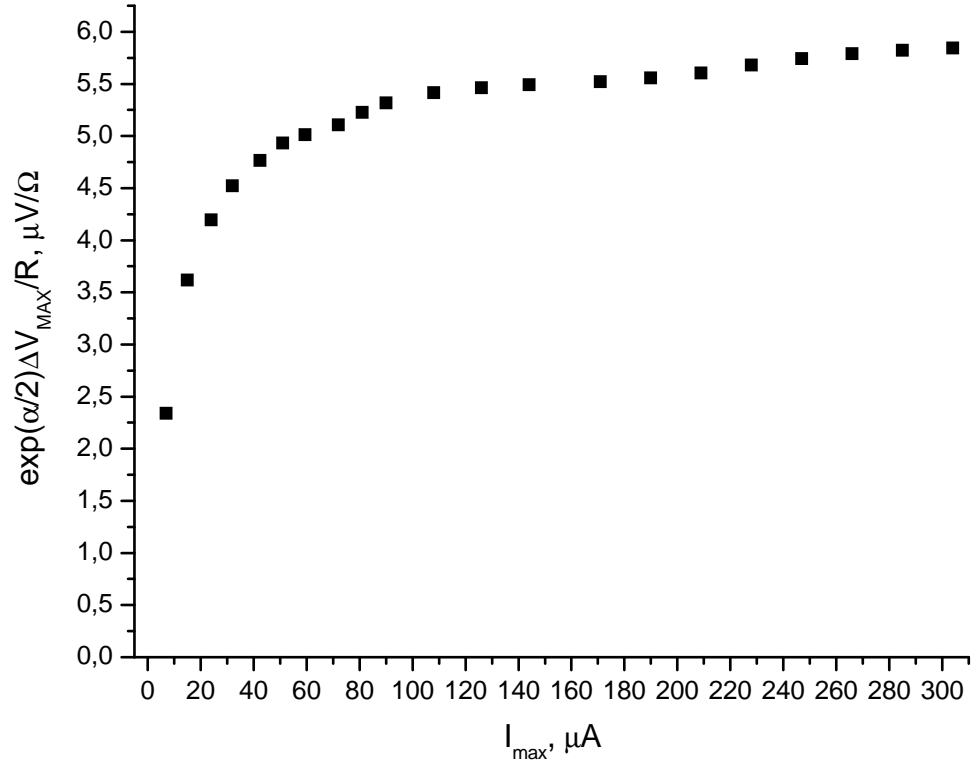


FIG. 4: Dependence of the maximum value of the reduced voltage modulation $\Delta V_{R,MAX}$ on the bias current I_{MAX} .

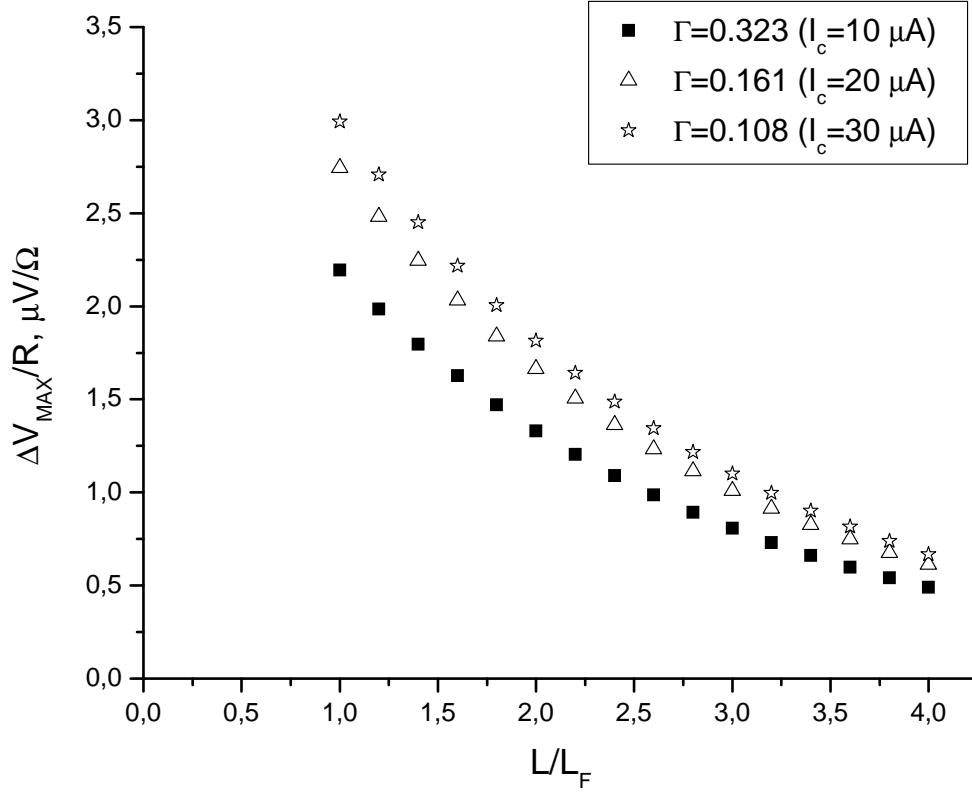


FIG. 5: The dependence of the maximum value of the voltage modulation $\Delta V_{MAX}/R$ on the inductance for symmetric DC SQUID; (black box)- $\Gamma = 0.323$ ($I_C = 10\mu A$); (triangle)- $\Gamma = 0.161$ ($I_C = 20\mu A$); (star)- $\Gamma = 0.108$ ($I_C = 30\mu A$).

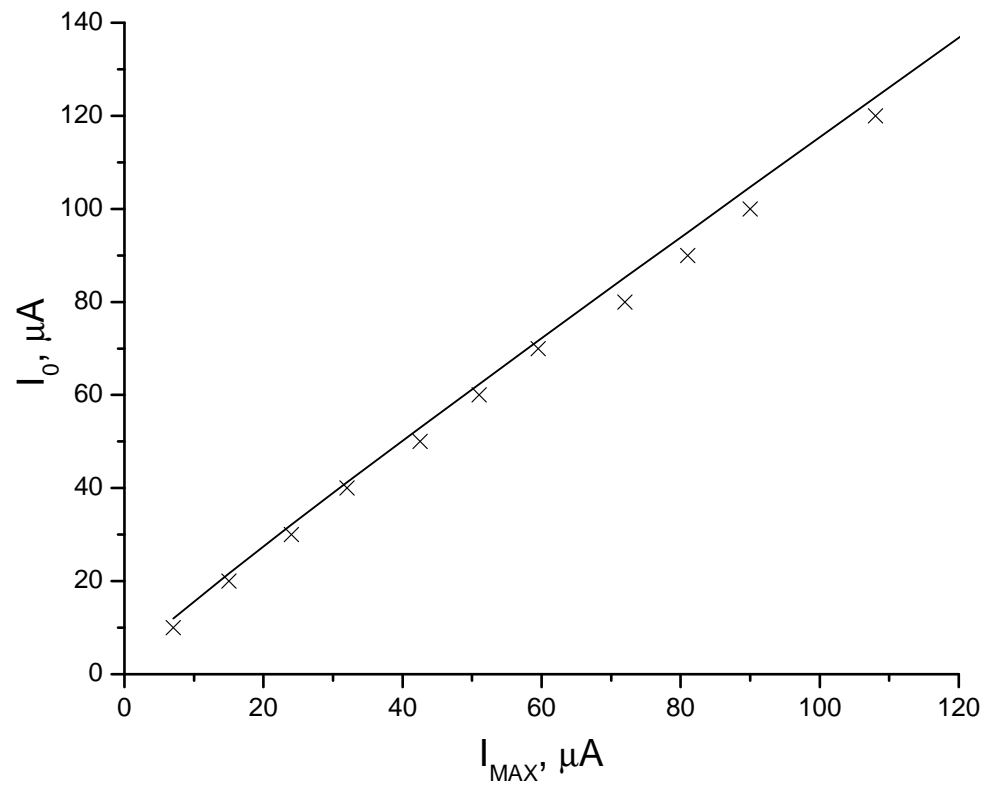


FIG. 6: The dependence of the SQUID critical current $I_0 = 2I_C$ on the bias current I_{MAX} . Solid line is the expression of Drung (Eq. (27)); crosses are theoretical points obtained from Eq. (11).

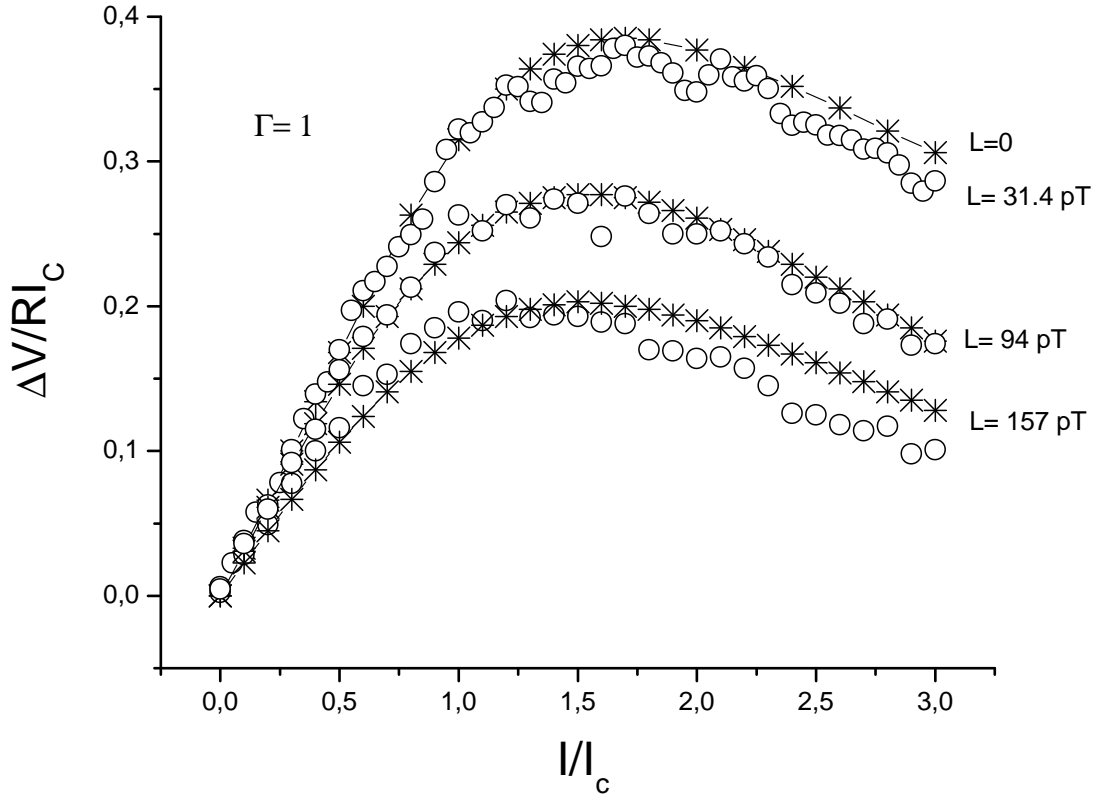


FIG. 7: The dependence of the normalized voltage modulation on the bias current. Comparison of theory (stars) with the simulation of Kleiner (opened circles). The curve for $L = 0$ was calculated from (7) and (8), the curves for $L = 94 \text{ pT}$, $L = 157 \text{ pT}$ were calculated from (11). All calculations are made at 77 K for $\Gamma = 1$.

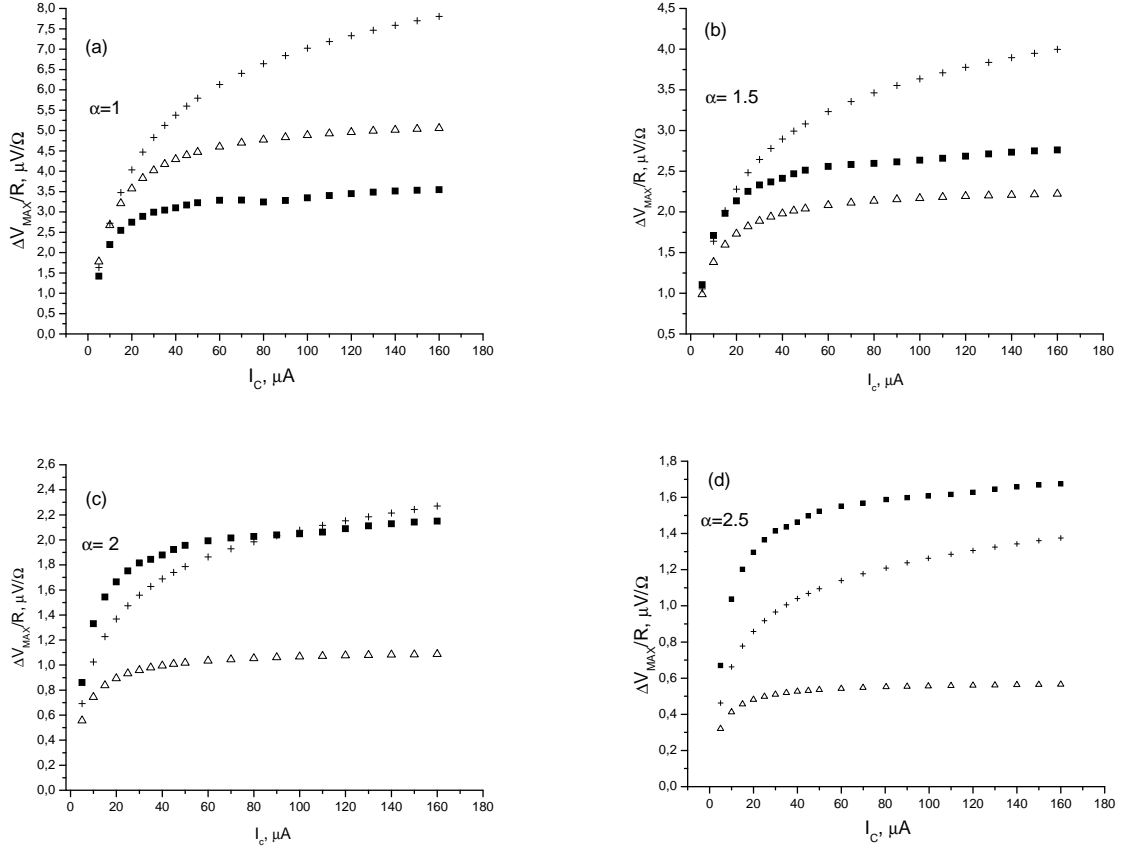


FIG. 8: The comparison of the maximum voltage modulation given by (Eq. (11)), (black box) with those obtained from the expressions of Kleiner (Eq. (28)), (cross) and Enpuku (Eq. (29)), (triangle) for: (a) $\alpha = 1$; (b) $\alpha = 1.5$; (c) $\alpha = 2$; (d) $\alpha = 2.5$.

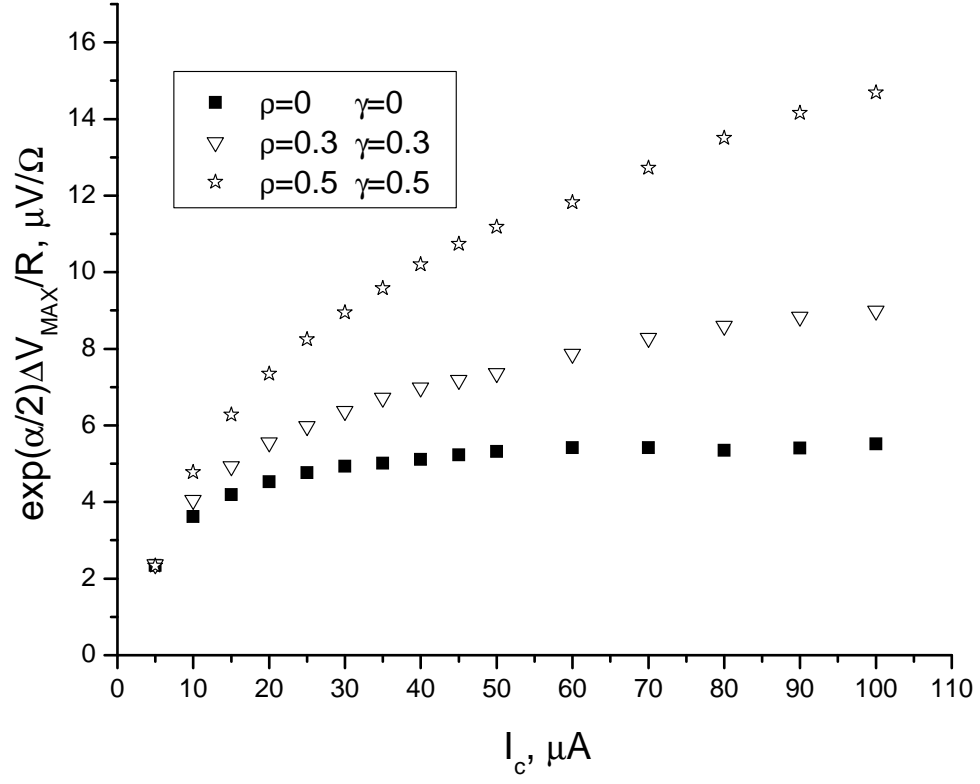


FIG. 9: The influence of the geometric asymmetry on the maximum voltage modulation, $\Delta V_{R,MAX}$.

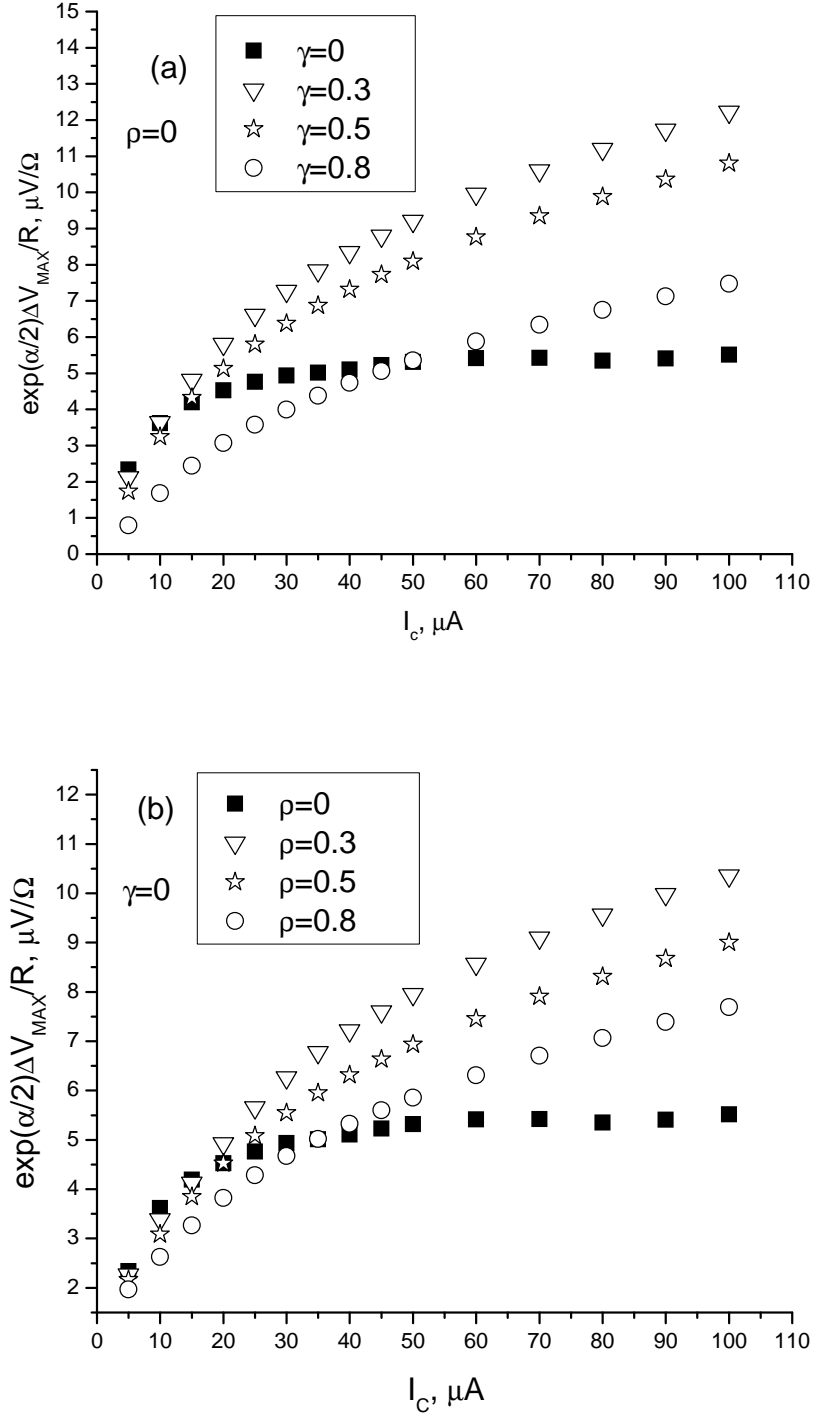


FIG. 10: The dependence of the maximum voltage modulation, $\Delta V_{R,MAX}$ on the critical current for two types of asymmetry: a) the current asymmetry ($\rho = 0$); b) the resistance asymmetry ($\gamma = 0$)

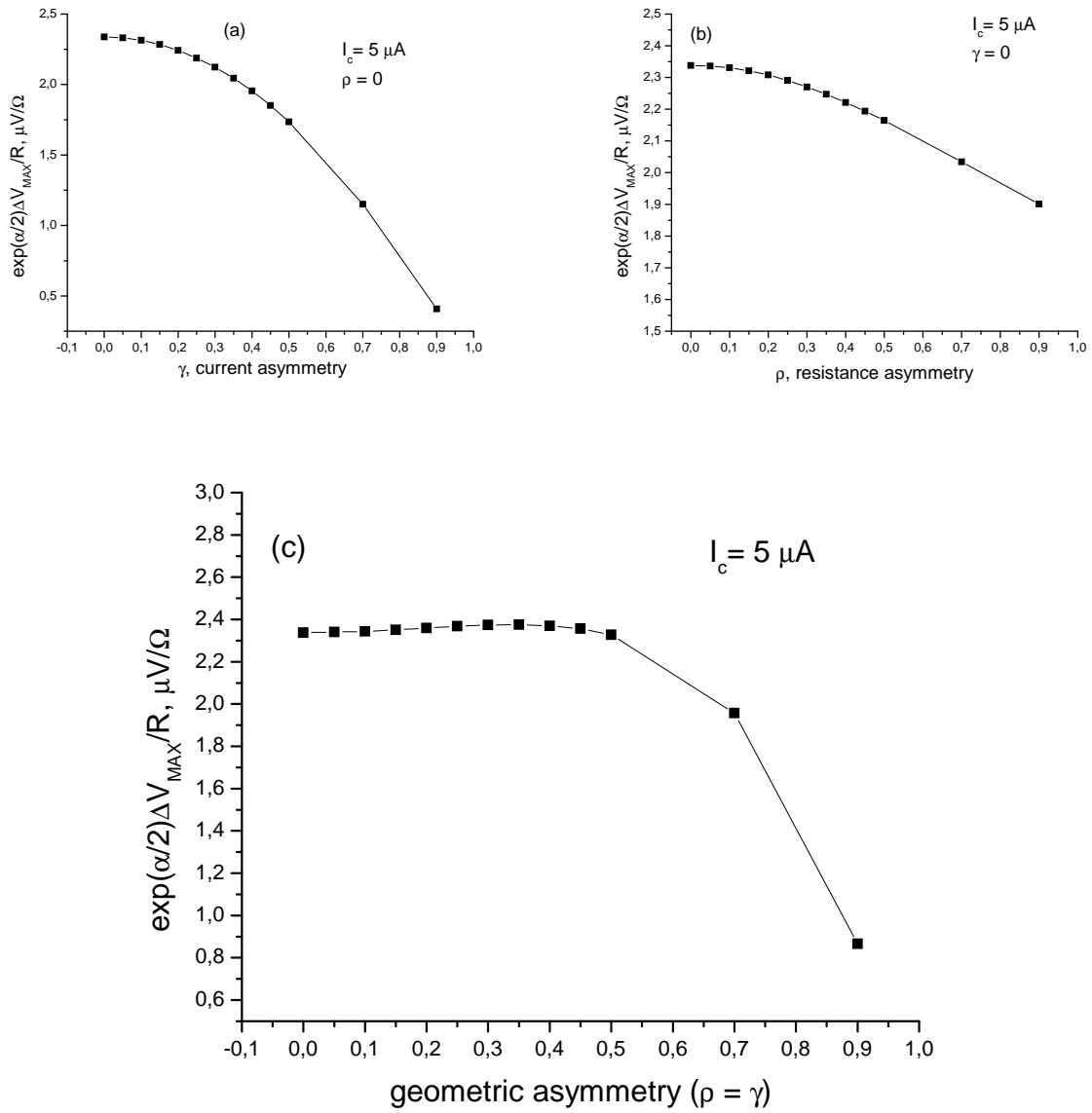


FIG. 11: The dependence of reduced maximum voltage modulation on the asymmetry parameters at $I_c = 5 \mu A$ for three types of asymmetry: a) $\rho = 0, \gamma \neq 0$; b) $\gamma = 0, \rho \neq 0$; c) $\rho = \gamma \neq 0$.

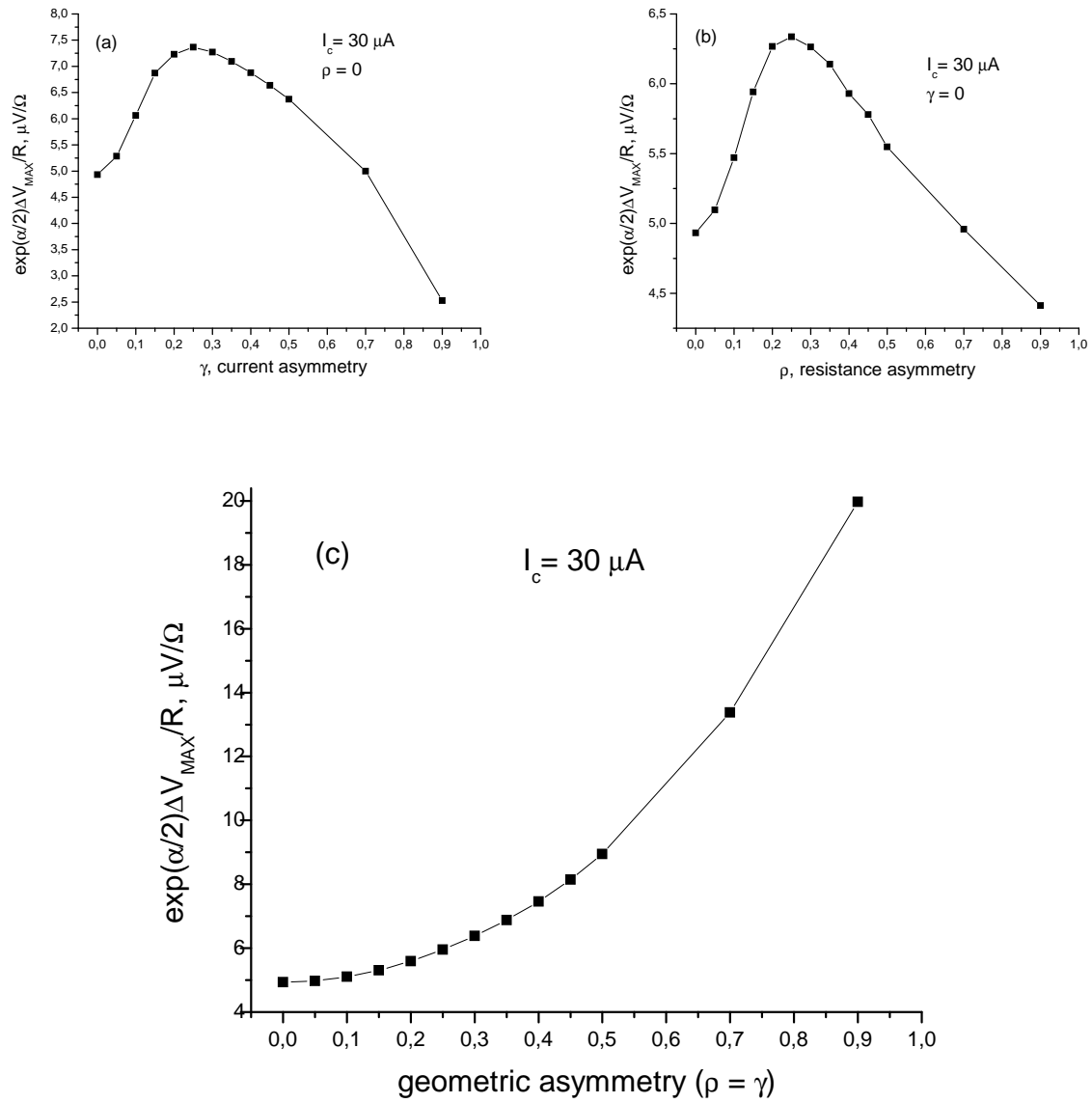


FIG. 12: The dependence of reduced maximum voltage modulation on the asymmetry parameters at $I_C = 30 \mu A$ for three types of asymmetry: a) $\rho = 0, \gamma \neq 0$; b) $\gamma = 0, \rho \neq 0$; c) $\rho = \gamma \neq 0$.

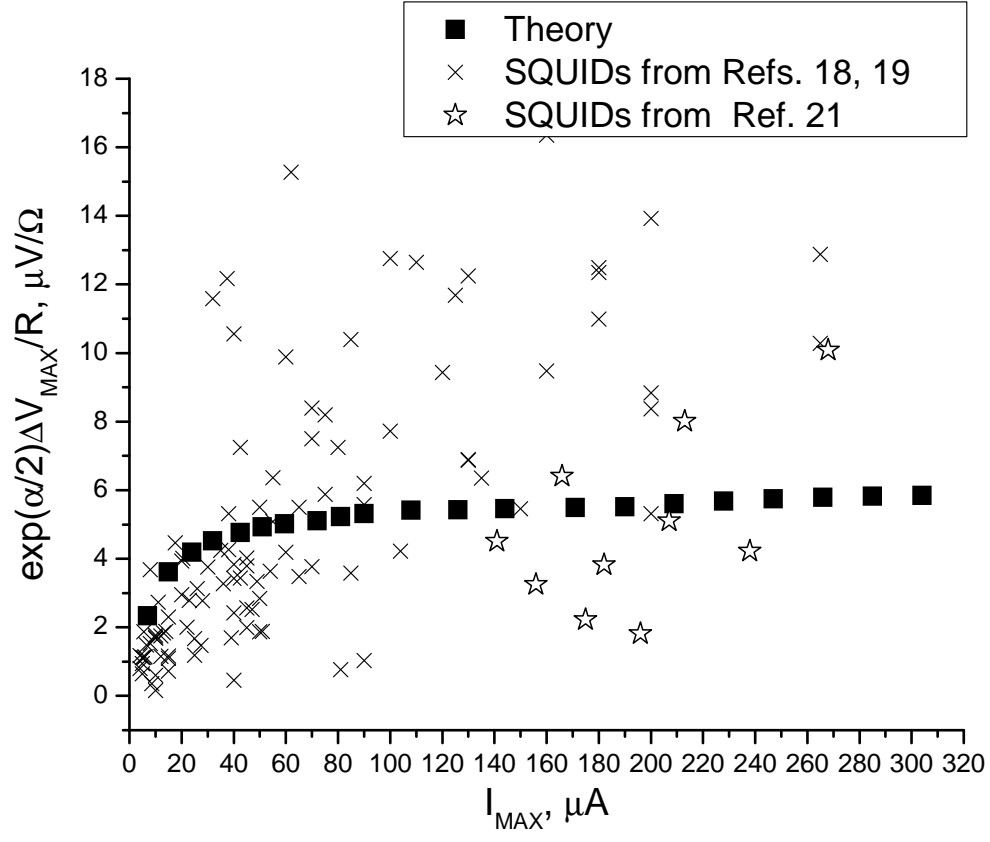


FIG. 13: The dependence $\Delta V_{R,MAX}(I_{MAX})$ for symmetric SQUID together with experimental points.

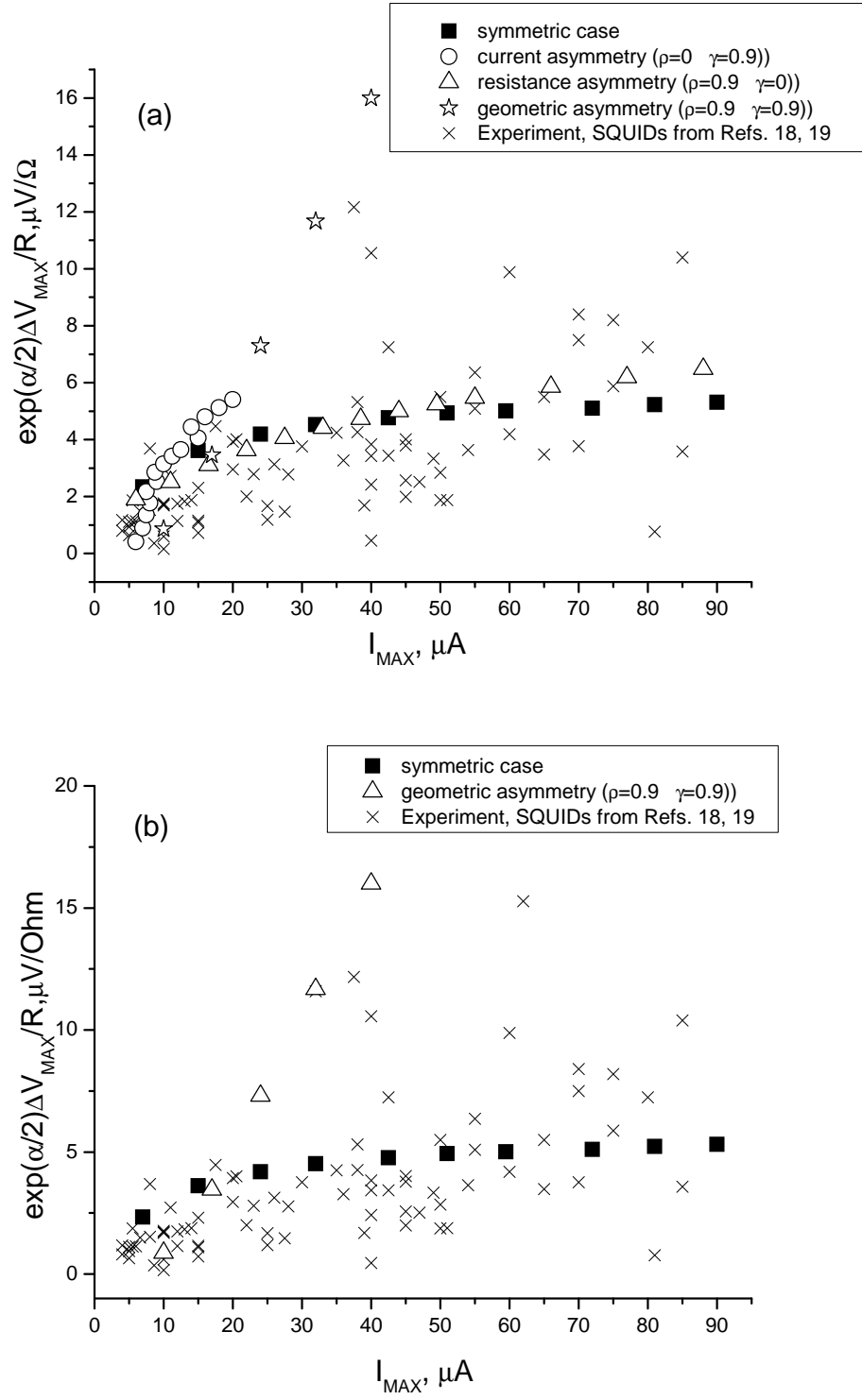


FIG. 14: The dependence $\Delta V_{R,MAX}(I_{MAX})$ for symmetric and asymmetric SQUIDs together with experimental points.